Nonlinear Kinetics of Glutamate Dehydrogenase. Studies with Substrates—Glutamate and Nicotinamide–Adenine Dinucleotide*

Janice S. Barton† and James R. Fisher‡

ABSTRACT: Substrate inhibition and substrate activation were observed with both glutamate and NAD using a 500-fold and a 3000-fold range of concentrations, respectively. Other investigators have reported substrate inhibition with glutamate and activation with NAD. We have confirmed these reports and in addition shown substrate inhibition with NAD and activation with glutamate. An empirical rate equation consisting of eight terms was deduced from a group of primary and secondary data plots. The kinetic constants in these terms were evaluated by the method of weighted least squares using a Control Data Corp. 6400 digital computer. The calculated lines were in very close agreement with the data and the standard error of calculated reciprocal velocity was 6% of the weighted average of the observed reciprocal velocity. It was shown that all eight terms are necessary to adequately define the experimental data. The empirical rate equation can be accounted for using random-substrate addition and product-release models with independent catalytic sites and without postulating second sites.

In living systems glutamic dehydrogenase (EC 1.4.1.3) provides an important pathway for incorporation of ammonia into carbon–nitrogen compounds. In view of this metabolic significance it is not surprising that the enzyme has been extensively studied. Early work by Olson and Anfinsen (1952) indicated that the associated molecule had a molecular weight of 1×10^6 and that it dissociated upon dilution. Coenzyme-induced dissociation was later reported by Frieden (1958) and at one time it was thought that the degree of association or dissociation had an important role in controlling enzymatic activity (Frieden, 1959a). This idea was revised when Fisher *et al.* (1962) demonstrated that the specific activity was constant over a 40-fold range of enzyme concentration, while the molecular weight changes by a factor of three. Subsequent studies have confirmed the activity of monomer (Frieden, 1963a) and have established that it has a molecular weight of 313,000 at infinite dilution (Eisenberg and Tomkins, 1968).

Kinetic studies of glutamic dehydrogenase from bovine liver have been numerous and the results often conflicting. This dehydrogenase is unusual, since it can catalyze the reaction using the coenzyme pair, NAD–NADH, or the phosphorylated pair, NADP–NADPH. According to Olson and Anfinsen (1952, 1953) who obtained the first highly purified crystalline enzyme, the nonphosphorylated pair is preferred. In addition, these authors reported that NAD, when used as a substrate gives nonlinear kinetics. Frieden (1959a) reported substrate activation with NAD but linearity with NADP whereas Eisenkraft and Veeger (1968) found substrate activation with NAD and substrate inhibition with NADP. Engel and Dalziel (1969) observed substrate activation with both NAD and NADP and in addition substrate inhibition with glutamate. Fahien and Strmecki (1969) did not observe substrate activation or inhibition with either NAD or NADP. Frieden (1959a) proposed a mechanism involving two coenzyme binding sites (only one was active) to explain the substrate activation kinetics but subsequently (Frieden, 1963b) reported no evidence for a second binding site. In addition, Yielding and Holt (1967) using equilibrium dialysis found no evidence for more than one NADH binding site per subunit. Furthermore, NADH binding had a simple dependence on NADH concentration and was independent of the enzyme concentration-dependent association.

The conflicting results and interpretations of the kinetic properties of this enzyme suggested that the mechanism may be more complex than previously thought. For this reason a careful and thorough investigation of the kinetic properties of the crystalline, ammonium sulfate suspended bovine liver glutamic dehydrogenase was undertaken. The results reported here confirm the more complex nature of this reaction. It was found that three substrates, NAD, NADP, and glutamate, exhibit substrate inhibition at high concentrations and substrate activation at lower concentrations. An empirical rate equation was deduced which describes these results. A random-pathway model with independent active sites that provide for the binding of one molecule of each substrate and product was found to be consistent with experimental data.

Materials and Methods

NAD and NADP were obtained from Sigma Chemical Co., and L-glutamic acid was purchased from Calbiochem. Gelman high-resolution buffer (Tris–barbital–sodium barbital) and cellulose polyacetate strips were bought from Gelman Instrument Co. A crystalline suspension of bovine liver glutamic dehydrogenase in 2.0 M ammonium sulfate was purchased from Calbiochem. This enzyme preparation was electrophoretically homogeneous at pH 8.8 and pH 7.5 in Gelman high-resolution buffer. The observed protein band was shown to be enzymatically active using the unstained halves of cellulose polyacetate strips. Filtered

* From the Department of Chemistry and Institute of Molecular Biophysics, Florida State University, Tallahassee, Florida. *Received August 6, 1970.* This work was supported by a contract with the Division of Biology and Medicine, United States Atomic Energy Commission and a grant from the National Science Foundation (GB-7293).

† Trainee in Biophysical Chemistry (U. S. Public Health Service GM-01776). Present address: Department of Biology, McCollum-Pratt Institute The Johns Hopkins University, Baltimore, Md.

‡ To whom inquiries should be addressed at Florida State University.

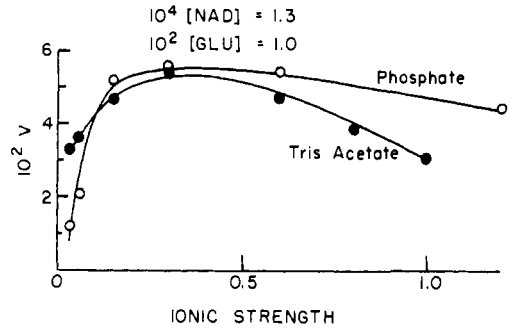

FIGURE 1: Plot of velocity (in optical density units per minute at 340 mμ) and ionic strength of buffer at constant NAD and glutamate concentrations. Phosphate buffer is represented by open circles and Tris–acetate by closed circles. Temperature 27°, pH 8, and enzyme concentration is 2.8 μg/ml.

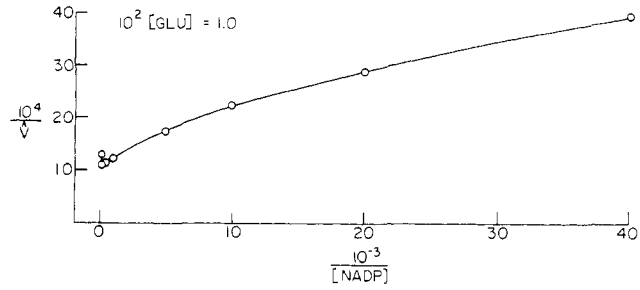

FIGURE 2: Double-reciprocal plot of velocity (measured at 340 mμ) and NADP concentration. Velocity is expressed in molecular activities in 0.1 M phosphate buffer at pH 8. Temperature is 27° and enzyme concentration is 2.8 μg/ml.

glass-distilled water was used in the preparation of all solutions.

Since this enzyme is unstable in dilute salt solutions (di Prisco and Strecker, 1966; Bitensky *et al.*, 1965) it was desirable to leave endogenous ammonium sulfate in the stored, dissolved, working solutions. Furthermore, it was necessary to include ammonium ions in the electrophoretic buffer in order to recover enzymatic activity.

Concentrations of NAD were calculated from absorbance measurements at 260 mμ using an extinction coefficient of 18×10^6 cm²/mole (Kornberg, 1957). Protein concentrations were determined using the method of Warburg and Christian (Warburg and Christian, 1941; Layne, 1957). A Gilford 2000 spectrophotometer with a variable chart speed of 0.25–12 in./min was used in measuring initial velocities at 340 mμ. Temperature was controlled by circulating water through the cell compartment with a Neslab water bath. Samples were preequilibrated to the reaction temperature in an insulated aluminum block compartmentalized to the size of 1-cm path-length cells. Water was circulated through this block and then into the cell compartment.

Conditions of assay were 0.1 M sodium phosphate buffer at pH 8, 1×10^{-4} M EDTA, and 27°. A standard assay at 5×10^{-2} M glutamate and 4.3×10^{-4} M NAD on the average gave a specific activity of 4.5 μmoles/min per mg of protein. Controls (standard assay) were run with each experiment and used to normalize all experimental values. Over a 2-year period all standard assays were within 15% of the value used for normalization. Initial velocities are reported as molecular activities ($\hat{V}$), *i.e.*, moles of NADH produced per minute per mole of enzyme using a molecular weight of 313,000. Ammonium sulfate from the enzyme preparation was diluted to a calculated concentration of 2.5×10^{-4} M in the reaction mixture. Twice this concentration was not inhibitory.

In this study initial velocities were found to be ionic strength dependent, causing a problem at high concentrations of glutamate. Results presented in Figure 1 indicate that velocity increases with ionic strength reaching a maximum at 0.3 ionic strength in Tris–acetate buffer. In phosphate buffer (Figure 1) maximum velocities occurred over a broader range of ionic strengths (0.2–0.6). This plateau in phosphate buffer permitted glutamic acid concentrations up to 0.1 M to be used in kinetic studies. Assuming an activity coefficient of one, the total ionic strength was maintained between 0.3 and 0.6. Similarly, Yielding and Tomkins (1962) found that velocity increased to a maximum as ionic strength was increased with sodium chloride.

The method of weighted least squares following Deming (1964) was used to obtain parameter values for the empirical substrate equation. Least-squares adjustments were carried out on the Control Data Corp. 6400 Computer, for which appropriate FORTRAN IV programs were written. Two subroutines for setting up and solving the matrices were kindly supplied by Dr. Delos DeTar. Except in the case of NADP, lines on all primary data plots were calculated from the empirical equation using the computer.

Results

Initial velocities were measured using NADP, NAD, and glutamate as the variable substrates and their double-reciprocal plots of velocity and concentration were qualitatively similar over the entire ranges investigated. At high concentrations the variable substrates exhibited inhibition while at lower values activation obtained.

The activation and inhibition displayed by NADP (Figure 2) are, broadly speaking, consistent with those described in the existing literature. Eisenkraft and Veeger (1968) observed inhibition, Frieden (1959b) linearity, and activation has been reported by di Prisco and Strecker (1969) and Engel and Dalziel (1969). These differences have been ascribed to the different reaction conditions used. However, the results in Figure 2 indicate that when a sufficiently wide range of NADP concentrations are used (1000-fold, 20–0.02 mM) all features can be seen under one set of conditions. Although Engel and Dalziel (1969) did cover wide concentration ranges, their highest concentration was only 0.05 the value we used which explains why they did not find substrate inhibition with NADP.

Substrate inhibition and activation results were obtained with glutamate and NAD when initial velocities were measured over a 500-fold and 3000-fold range of concentrations, respectively. Typical results (over limited ranges) found with NAD and glutamate are shown as double-reciprocal plots in Figures 3 and 4. The upward curvature at very high concentration is typical of substrate inhibition (Figure 3). Generally, this is expressed mathematically by including terms first order in substrate concentration (*e.g.*, $1/\hat{V} = \ldots + a[\text{Glu}]$). Commonly used random-addition models and dead-end branched models can yield such terms (*e.g.*, Wong and Hanes, 1962; Cleland, 1963; Fisher and Hoagland, 1968). Activation by both substrates is recognizable by the downward curvature at lower concentrations (Figure 4).

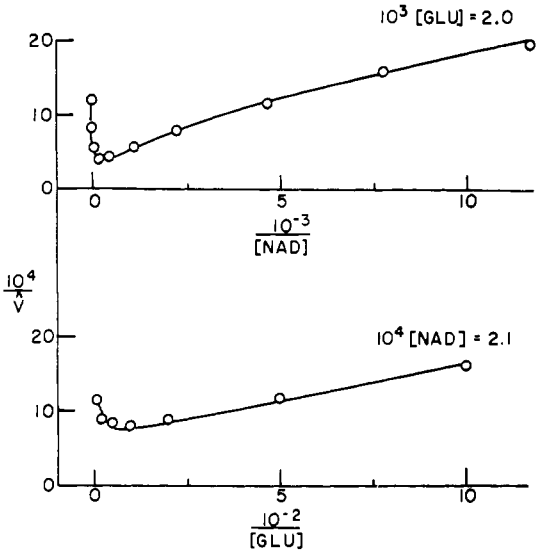

FIGURE 3: Double-reciprocal plots of velocity and NAD concentration (upper half) and glutamate concentration (lower half) showing substrate inhibition. Assay conditions are the same as in Figure 2. Lines are calculated as stated in the text.

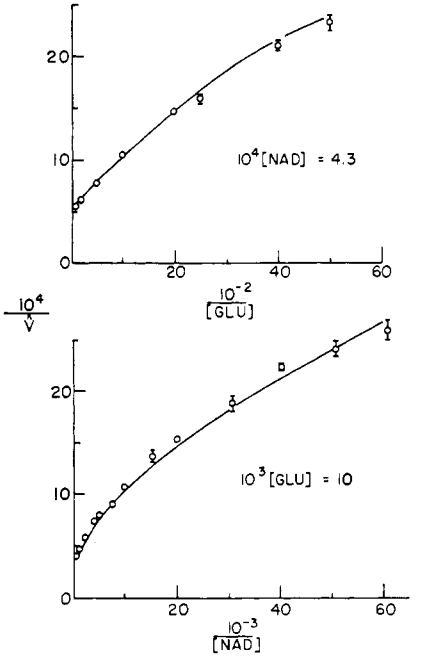

FIGURE 4: Double-reciprocal plots of velocity and substrate concentration showing substrate activation with glutamate (upper half) and with NAD (lower half). See Figure 2 for conditions. Lines are calculated as stated in text.

Curvature of this type is expressible mathematically by the following simple function, which is predicted by several kinetic models currently in use. Random-addition models

$$1/\hat{V} = \ldots + \frac{1}{a + b[\text{Glu}]}$$

used by Cleland (1963), Wong and Hanes (1962), and Fisher and Hoagland (1968) and second-site models of the kind used by Frieden (1959a) to explain the activation kinetics of glutamic dehydrogenase will yield this term. Also, models involving negative cooperativity can reduce to such a function (Dalziel and Engel, 1968).

In order to develop an empirical rate equation, the substrate curves were divided into two parts consisting of substrate activation and inhibition. Each part was analyzed separately for the terms primarily responsible for the shapes of the primary and secondary plots. The terms for each section were then appropriately combined into one equation. In the next section the term or terms that describe the experimental curves will be presented, followed by a justification for their appearance in the rate equation.

Substrate Inhibition with Glutamate. Glutamate inhibition was studied over a 30-fold range of NAD concentrations. In Figure 5 substrate inhibition (where the reciprocal of velocity is a direct function of substrate concentration) is shown for glutamate. Slopes and intercepts were obtained from the straight-line portions of the experimental curves. When the intercepts and their reciprocals were plotted as functions of the reciprocal and the direct concentrations of NAD, the resulting lines were all nonlinear. These intercepts are shown in Figure 6A as a function of reciprocal NAD concentrations. Careful consideration of the primary and secondary plots led to the conclusion that two terms, $I = a/[\text{NAD}] + 1/(b + c[\text{NAD}])$, were the simplest combination that would predict the data in Figure 6A. These terms are the primary contributors to the intercept which has two limiting forms. At low NAD concentrations the intercept reduces to $I_1 = a/[\text{NAD}] + 1/b$, which defines the limiting line approached as NAD decreases. The straight line described by $I_2 = (a + 1/c)/[\text{NAD}]$ is approached at high NAD concentrations. Notice that the slope of reciprocal NAD for I_2 is greater than the corresponding slope for I_1 which is in agreement with experimental data, since in Figure 6A the limiting line at high NAD has a greater slope than the limiting line at low NAD.

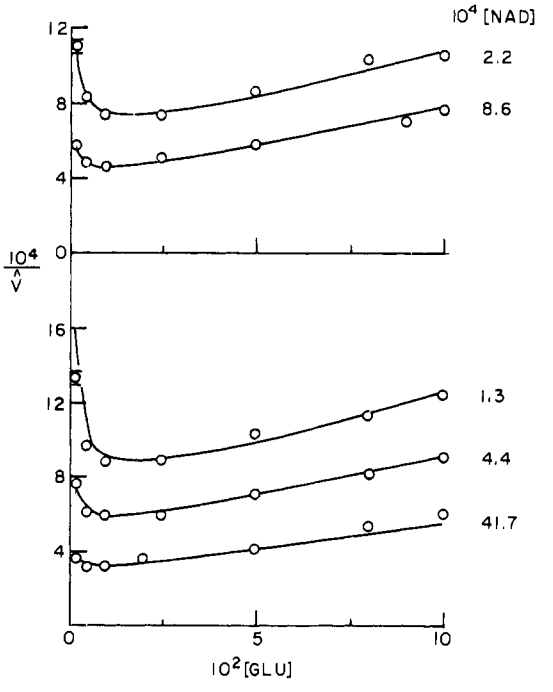

FIGURE 5: A plot of reciprocal velocity *vs.* glutamate concentration at several NAD concentrations (given in figure) in the substrate inhibited region. See Figure 2 for conditions. Lines are calculated as stated in the text.

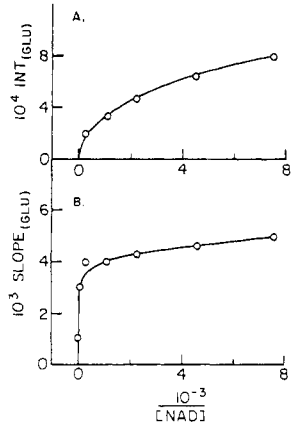

FIGURE 6: Secondary plots of the data in Figure 5 with intercepts (A) and slopes (B) plotted as functions of reciprocal NAD concentrations.

The high glutamate slopes and their inverses were found to be nonlinear functions of NAD and its reciprocal. Figure 6B contains a plot of slopes of glutamate *vs.* reciprocal NAD concentrations. The slope at low NAD appears to be linear but at very high NAD concentrations there is an abrupt downward deflection. These results can be described by the terms: $d/[NAD] + 1/(e + f[NAD])$. The logic used to deduce these terms closely followed the analysis of the high glutamate intercept data. For example, the limiting line approached at low NAD is $d/[NAD] + 1/e$ while at high NAD, $(d + 1/f)/[NAD]$ describes the limiting line. These terms at high and low NAD are implicit in the terms given above. All data in the substrate inhibited region of glutamate are accounted for by the four terms in eq 1.

$$\frac{1}{\hat{V}} = \frac{a}{[NAD]} + \frac{1}{b + c[NAD]} + \frac{d[Glu]}{[NAD]} + \frac{[Glu]}{e + f[NAD]} \quad (1)$$

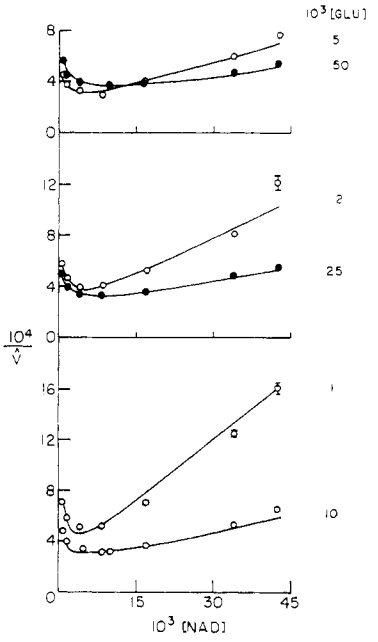

FIGURE 7: The reciprocal of velocity is plotted against NAD concentrations at several glutamate concentrations (given in figure) in the NAD substrate inhibited region. See Figure 2 for conditions. Lines are calculated as stated in the text.

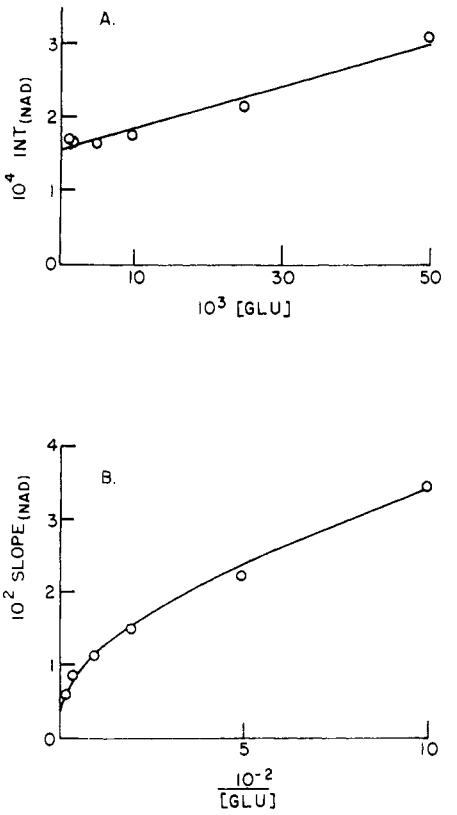

FIGURE 8: Secondary plots of the data in Figure 7 with intercepts (A) plotted as a function of glutamate concentration and slopes (B) as a function of reciprocal glutamate concentration.

Substrate Inhibition with NAD. The substrate inhibited region of NAD was investigated over a 50-fold concentration range of glutamate and the results are given in Figure 7. Again, slopes and intercepts were obtained from the straight-line portions of the data. In all combinations the slopes and reciprocal slopes at high NAD were plotted against the direct and reciprocal concentrations of glutamate. In every case the resulting lines were nonlinear. Figure 8B shows the result of plotting the slope *vs.* reciprocal glutamate concentrations. The basic shape of the curve is predicted by the terms $g/[Glu] + 1/(h + i[Glu])$. The limiting line approached at low glutamate is accounted for by $g/[Glu] + 1/h$, while the line approached at high glutamate is $(g + 1/i)/[Glu]$. These two limiting forms predict the slope of the limiting line at high glutamate to be greater than the one at lower glutamate concentrations. Results in Figure 8B and these predictions are consistent.

The intercepts at high NAD concentrations are approximated by a linear function of glutamate *i.e.*, $a + b[Glu]$. In the previous section (Substrate Inhibition with Glutamate), two terms with glutamate in the numerator were presented and justified. It was found that one of these terms $[Glu]/(e + f[NAD])$ would also account for the glutamate dependence of the intercept, and that the other term was negligible at all glutamate concentrations used in NAD substrate inhibition studies. This term is negligible at low glutamate but does become important at higher concentrations. Consequently, to account for the intercept at high NAD, it was necessary to bring in only one new term—a constant—to obtain the form required by the secondary plot. Reciprocal velocities in the substrate-inhibited region of NAD are predicted by eq 2.

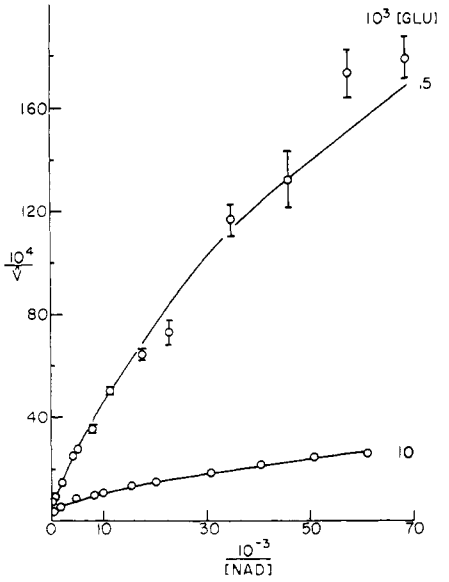

FIGURE 9: Double-reciprocal plots of velocity and NAD concentrations at two glutamate concentrations (given in figure) in the substrate activation region of NAD. See Figure 2 for conditions. Lines are calculated as stated in text.

$$\frac{1}{\hat{V}} = j + \frac{[\text{Glu}]}{e + f[\text{NAD}]} + \frac{g[\text{NAD}]}{[\text{Glu}]} + \frac{[\text{NAD}]}{h + i[\text{Glu}]} \quad (2)$$

Seven terms that will calculate all reciprocal velocities in the inhibition range of both substrates result from an appropriate combination of eq 1 and 2

$$\frac{1}{\hat{V}_{SI}} = \frac{a}{[\text{NAD}]} + \frac{1}{b + c[\text{NAD}]} + \frac{d[\text{Glu}]}{[\text{NAD}]} + \frac{[\text{Glu}]}{e + f[\text{NAD}]} + \frac{g[\text{NAD}]}{[\text{Glu}]} + \frac{[\text{NAD}]}{h + i[\text{Glu}]} + j \quad (3)$$

where $1/\hat{V}_{SI}$ = reciprocal velocities in the substrate-inhibited ranges with either or both substrates.

Substrate Activation with Glutamate and NAD. Results presented in Figures 9–11 are typical of activation obtained with glutamate and NAD. For both substrates, velocity and its inverse were plotted against the varied substrate and its reciprocal. All combinations were plotted and found to be nonlinear. The simplest type of term that will account for the shape of the curves for either NAD or glutamate has the form $1/(a + b[\text{NAD}])$ or $1/(a + b[\text{Glu}])$.

It seemed reasonable that one term might account for the activation effect of both substrates. The term of eq 4 has this capability, and it is apparent when either substrate is held constant, it reduces to the simple forms suggested above.

$$\frac{1}{\hat{V}_{SA}} = \frac{1}{k[\text{NAD}] + l[\text{Glu}] + m[\text{NAD}][\text{Glu}]} \quad (4)$$

$1/\hat{V}_{SA}$ = reciprocal velocities in the substrate-activated ranges with either or both substrates and

$$\frac{1}{\hat{V}} = \frac{1}{\hat{V}_{SI}} + \frac{1}{\hat{V}_{SA}} \quad (5)$$

The kinetic coefficients in eq 3 were evaluated by the methods of weighted least squares and $1/\hat{V}_{SI}$ calculated in the substrate-activated regions. Using eq 5, $1/\hat{V}_{SA}$ was obtained by subtraction for each experimental reciprocal velocity. When $1/\hat{V}_{SA}$ was plotted *vs.* the reciprocal of either glutamate or NAD concentration, curved lines resulted like these in Figures 9–11 except that all lines passed through the origin. Straight lines resulted when $\hat{V}_{SA}$ was plotted against the concentrations of either substrate (Figures 12 and 13). Any term proposed for the substrate activation data must account for the linearity of the data in Figures 12 and 13 and the observed dependence of each slope and intercept on the second substrate. When eq 4 is inverted eq 6 results, which is consistent with the above requirements. On this basis it was concluded that the substrate

$$\hat{V}_{SA} = k[\text{NAD}] + l[\text{Glu}] + m[\text{NAD}][\text{Glu}] \quad (6)$$

activation data are accounted for by the single term in eq 4. Equations 3 and 4 were combined to form eq 7, which describes all the data over the entire glutamate and NAD con-

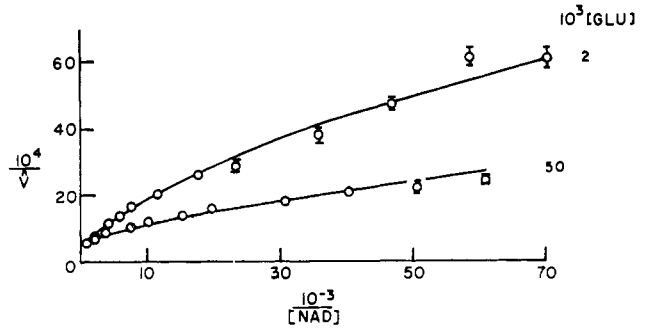

FIGURE 10: Double-reciprocal plots of velocity and NAD concentration at two glutamate concentrations (given in figure) in the substrate-activation region of NAD. See Figure 2 for conditions. Lines are calculated as stated in text.

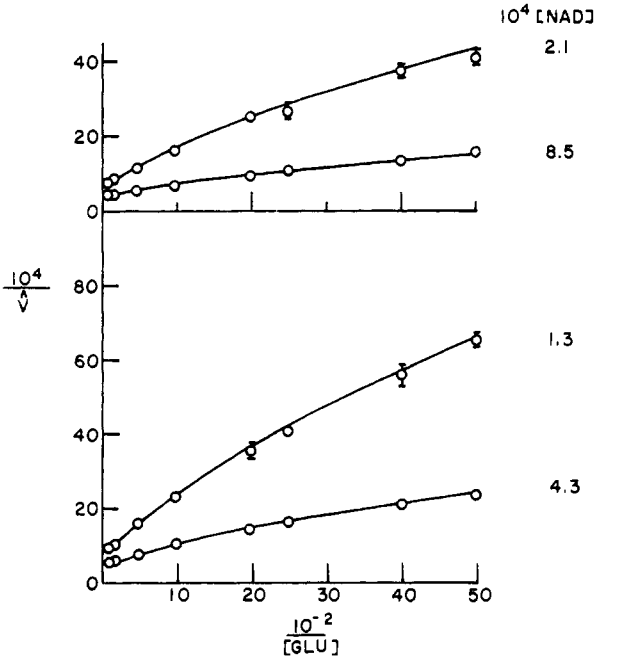

FIGURE 11: Double-reciprocal plots of velocity and glutamate concentration at four NAD concentrations (given in figure) in the substrate-activation region of glutamate. See Figure 2 for conditions. Lines are calculated as stated in text.

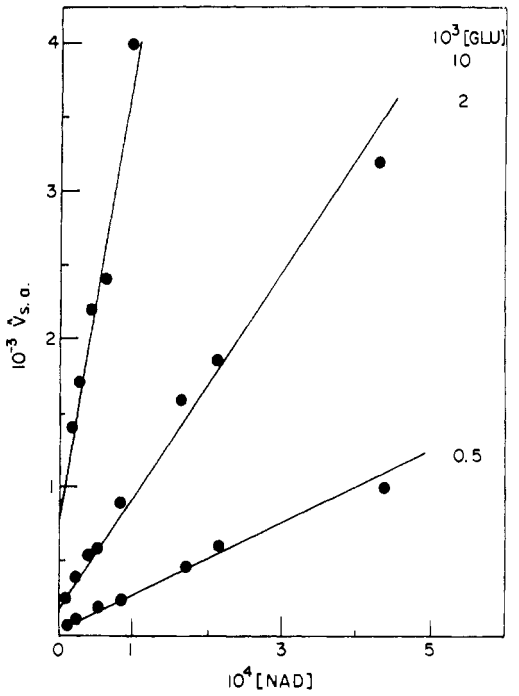

FIGURE 12: A plot of the $\hat{V}_{SA}$ *vs.* NAD concentration at several glutamate concentrations (given in figure).

centration ranges investigated using the parameter values given in Table I. Each term is identified by a Roman numeral

$$\frac{1}{\hat{V}} = \underbrace{\frac{a}{[\mathrm{NAD}]}}_{\mathrm{I}} + \underbrace{\frac{1}{b + c[\mathrm{NAD}]}}_{\mathrm{II}} + \underbrace{\frac{d[\mathrm{Glu}]}{[\mathrm{NAD}]}}_{\mathrm{III}} + \underbrace{\frac{[\mathrm{Glu}]}{e + f[\mathrm{NAD}]}}_{\mathrm{IV}} + \underbrace{\frac{g[\mathrm{NAD}]}{[\mathrm{Glu}]}}_{\mathrm{V}} + \underbrace{\frac{[\mathrm{NAD}]}{h + i[\mathrm{Glu}]}}_{\mathrm{VI}} + \underbrace{j}_{\mathrm{VII}} + \underbrace{\frac{1}{k[\mathrm{NAD}] + l[\mathrm{Glu}] + m[\mathrm{NAD}][\mathrm{Glu}]}}_{\mathrm{VIII}} \quad (7)$$

for later reference. A total of 160 different combinations of NAD and glutamate concentrations was used in the evaluations of these parameters and each experimental point was an average of at least 6 determinations. In some cases (very low velocities) 9 replicates were used, which means that over 1000 experimental points were used in the evaluation of eq 7. The lines drawn in Figures 3–5, 7, and 9–11 were calculated using eq 7 and the constants in Table I. The standard error of reciprocal velocity was 6% of the weighted average of observed reciprocal velocities.

Analysis of the Empirical Rate Equation. Although the terms of the substrate empirical rate equation (eq 7) were deduced by analysis of secondary data plots, the criteria for including any terms in the equation must also take into account the reproducibility of all the primary data and the standard error of calculated reciprocal velocity. The latter, of course, is the square root of the sum of weighted squares of the residuals divided by the degrees of freedom ($N - P$) and the average weight of reciprocal velocity ($W_{1/\hat{V}}$) and is a statistic indicating the closeness of fit (see below). The "i" represents and experimental point, "N" the total number of points, "P" the number of adjustable parameters, and

$$\text{"}W\text{"}_{1/\hat{V}} = \left(\sum_i^N W_i\right)\Big/N$$

$$(\text{std error of } 1/\hat{V}_{\text{calcd}})^2 = \sum_i^N \frac{W_i(1/\hat{V}_{\text{obsd }i} - 1/\hat{V}_{\text{calcd }i})^2}{(N - P)W_{1/\hat{V}}}$$

TABLE I: Weighted Least-Squares Values of Kinetic Constants in Equation 7.

Constant	Value[a]
a	$(1.9 \pm 0.3) \times 10^{-8}$
b	$(2.3 \pm 0.2) \times 10^{3}$
c	$(3.8 \pm 0.6) \times 10^{6}$
d	$(2.0 \pm 0.7) \times 10^{-7}$
e	$(2.6 \pm 0.3) \times 10^{2}$
f	$(3.0 \pm 0.8) \times 10^{4}$
g	$(2.7 \pm 0.2) \times 10^{-5}$
h	$(1.6 \pm 0.1) \times 10^{2}$
i	$(2.1 \pm 1.3) \times 10^{2}$
j	$(1.91 \pm 0.01) \times 10^{-4}$
k	$(4.4 \pm 1.0) \times 10^{5}$
l	$(6.6 \pm 1.4) \times 10^{4}$
m	$(3.8 \pm 0.3) \times 10^{9}$

[a] Standard deviation of the constants based on reciprocal velocity standard error of 2.5×10^{-5} which is 6% of the weighted average of reciprocal velocity of 4.4×10^{-4}.

To ensure that we had developed the simplest equation that would give an acceptable fit to the data and that the number of terms in the rate equation was on the conservative side, the following analysis was completed. Each of the eight terms of eq 7 was omitted from the operating rate equation and using the weighted least-squares program, the computer was instructed to find the best values of the kinetic coefficients, to calculate reciprocal velocities, and to compute a standard error of calculated reciprocal velocity. The reproducibility of the data and the standard error obtained when a term was omitted was then compared to results found with the entire empirical rate equation. The results summarized in Table II show that positive kinetic coefficients were only found when terms V and VII were left out. Although convergence occurred when the other six terms were omitted, at least one coefficient was negative in every case.

Focusing attention on terms V and VII which did give all positive coefficients, we observe that the standard error is 20% greater than the value calculated with eq 7 when term VII is omitted and it is 80% greater when term V is removed. A question might be raised concerning the significance of the 20% increase exhibited with term VII removed. When calculated velocities obtained in its absence were plotted on the same graph with those resulting when eq 7 was used, the poorer fit was obvious. The calculated lines (with term VII omitted) were outside the experimental standard deviations of the mean for many points. It is clear from the above analysis that eq 7 is a markedly superior description of the data than the equation resulting when any one of the eight terms was omitted.

The activation term (VIII) is not the least complex that might predict the values of $1/\hat{V}_{SA}$ (defined in previous section).

TABLE II: Results of Omitting Terms from Equation 7.

	Term Omitted	Std Error × 10^5	Comment
I	$\frac{a}{[NAD]}$	2.60	Neg coefficient[a]
II	$\frac{1}{b + c[NAD]}$	3.35	Neg coefficient
III	$\frac{d[Glu]}{[NAD]}$	2.46	Neg coefficient
IV	$\frac{[Glu]}{e + f[NAD]}$	3.78	Neg coefficient
V	$\frac{g[NAD]}{[Glu]}$	4.39	Pos coefficients
VI	$\frac{[NAD]}{h + i[Glu]}$	3.39	Neg coefficient
VII	j	3.01	Pos coefficients
VIII	$\frac{1}{k[NAD] + l[Glu] + m[NAD][Glu]}$	13.63	Neg coefficient
	None	2.49	Pos coefficients

[a] Negative coefficient means that one or more coefficients in the remaining terms are negative. In every case efforts have been made to obtain convergence with all positive values by holding various coefficients constant and allowing the others to be adjusted.

For mathematical and statistical comprehensiveness, four plausible alternatives were substituted for term VIII. The best kinetic coefficient values and the standard error were calculated with each alternative using the computer. As seen in Table III when convergence did occur the standard error exceeded that given by eq 7, and furthermore, at least one coefficient was negative in value. A solution could not be found when the third term of Table III was substituted for term VIII.

Discussion

The steady-state kinetic properties of bovine liver glutamic dehydrogenase have been studied by a variety of investigators over many years. There seems to be general agreement that NAD gives substrate activation nonlinearity (Frieden, 1959a; Eisenkraft and Veeger, 1968; Engel and Dalziel, 1969) and in addition Engel and Dalziel (1969) observed substrate inhibition with glutamate. We have confirmed these observations and have shown substrate activation nonlinearity with glutamate as well as substrate inhibition with NAD and NADP. While glutamate does not give as extensive nonlinearity in the substrate-activation range as does NAD there seems no doubt that there is a very significant and reproducible downward bend in reciprocal plots. It should be noted that some of the kinetic features observed by others were found under differing conditions of pH and buffer concentration. In the studies reported here, it is clear that all of these kinetic features occur under one set of conditions wherein changes in ionic strength are not a factor.

TABLE III: Possible Alternative Activation Terms.

Term No.	Term Substituted	Std Error × 10^5	Comment
1	$\frac{1}{[Glu]\,(a + b[NAD])}$	2.52	Neg coefficient[a]
2	$\frac{1}{a + b[NAD][Glu]}$	5.66	Neg coefficient
3	$\frac{1}{a + b[Glu]}$		Not converge
4	$\frac{1}{a[NAD] + b[Glu]}$	7.3	Neg coefficient

[a] See footnote to Table II.

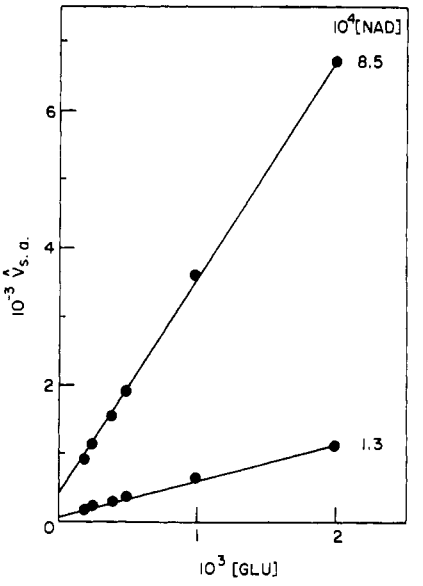

FIGURE 13: A plot of $\hat{V}_{SA}$ *vs.* glutamate concentration at two NAD concentrations.

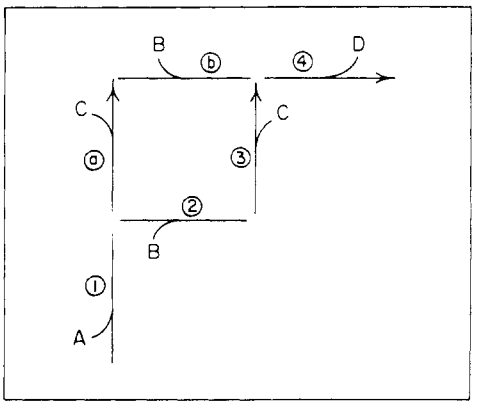

FIGURE 14: A simple random-pathway model from which activation terms can be generated. Steps a, 3, and 4 are considered irreversible because products (C and D) are omitted and initial velocities are measured.

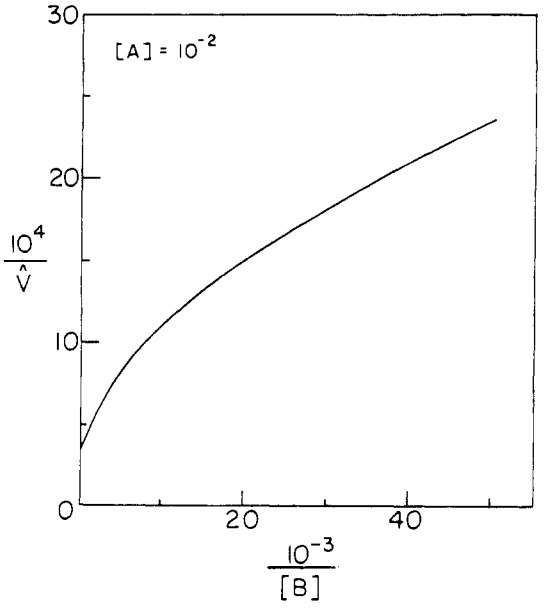

FIGURE 15: Activation curve (in Lineweaver–Burk form) calculated from the model of Figure 14 and the rate constants in Table IV. $\hat{V}$ is moles/minute per mole of enzyme.

Since it is not feasible to present all experimental data accumulated during extensive kinetic studies, it seems desirable to summarize it with an empirical rate equation, particularly, if it does not restrict the kinds of models that can be used for interpretation. In this connection it should be noted that the various terms in the empirical equation presented (eq 7) are readily deducible from random models, multiple-site models, and negative-cooperativity models. The only possible exception may occur with the negative-cooperativity model, since we have not seen this model used to interpret both substrate inhibition and substrate activation with the same system; however, it may be possible to do so.

We have chosen to interpret our data using random-addition models for a variety of reasons (Barton, 1970). Evidence presented to date seems to preclude multiple binding site models for NAD. Frieden (1963b) did not find evidence for more than one NAD binding site on glutamic dehydrogenase which is consistent with the studies of Yielding and Holt (1967) wherein they report only one binding site per subunit for NADH. In addition, these studies show linear Scatchard plots with NADH indicating the lack of site–site interactions in this system. These results do not favor the negative-cooperativity models that have been suggested (Dalziel and Engel, 1968; Engel and Dalziel, 1969). Since random-addition models can readily explain all of these results without postulating multiple sites, or site–site interactions, or any other special conditions, we feel they are the simplest models available and that they should be used for interpreting kinetic data, unless there is specific evidence for more complex models. In the following section a simple random model is used to show how substrate activation curves can be generated and combined with substrate inhibition.

Sweeny and Fisher (1968) used a simple random model to generate sigmoid data and we thought it would demonstrate the flexibility of random models to use this same one with different rate constants to generate substrate-activation curves. This model is shown in Figure 14 and the rate constants used in Table IV. It should be noted that all of the values fall in the normal range of observed rate constants (Eigen and Hammes, 1963). The calculated substrate-activation curve for this model is presented in Figure 15 and is fully compatible in general shape with the experimental data shown in the previous section (compare with the lower curve in Figure 4). Furthermore, it is easy to incorporate substrate inhibition into this model by simply adding a dead-end branch and with an appropriate binding constant a curve showing substrate activation and substrate inhibition can be readily generated. It should be emphasized that in the model being used here only one substrate can give a nonlinear reciprocal plot, and, therefore, is not being suggested as a specific model for the glutamic dehydrogenase system. Rather it is being used to show that random models, in general, can deal with the kinds of kinetic properties exhibited by the glutamic dehydrogenase system. General random-addition models have been generated and specific ones identified which can deal with all of the data contained in this report (Barton, 1970). The details of these theoretical interpretations will be the subject of a later report.

TABLE IV: Rate Constant Assignments for the Model in Figure 14.[a]

First-Order Rate Constants	min^{-1}	Second-Order Rate Constants	M^{-1} min^{-1}
k_{-1}	10^3	k_1	10^6
k_{-2}	10^3	k_2	10^7
k_a	10^3	k_b	10^9
k_3	10^5		
k_{-b}	8×10^4		
k_4	4×10^3		

[a] [A] = 10^{-2}; [B] is variable substrate.

Acknowledgments

We thank Dr. Delos DeTar for his invaluable help in developing the computer programs and Mrs. Janet Nickels for her expert technical assistance.

References

Barton, J. S. (1970), Ph.D. Dissertation, Florida State University, Tallahassee, Fla.
Bitensky, M. W., Yielding, K. L., and Tomkins, G. M. (1965), *J. Biol. Chem. 240*, 1077.
Cleland, W. W. (1963), *Biochim. Biophys. Acta 67*, 104.
Dalziel, K., and Engel, D. C. (1968), *FEBS (Fed. Eur. Biochem. Soc.) Lett. 1*, 349.
Deming, W. E. (1964), Statistical Adjustment of Data, New York, N. Y., Dover.
di Prisco, G., and Strecker, H. J. (1966), *Biochim. Biophys. Acta. 122*, 413.
di Prisco, G., and Strecker, H. J. (1969), *Eur. J. Biochem. 9*, 507.
Eigen, M., and Hammes, G. G. (1963), *Advan. Enzymol. 25*, 1.
Eisenberg, H., and Tomkins, G. M. (1968), *J. Mol. Biol. 31*, 37.
Eisenkraft, B., and Veeger, C. (1968), *Biochim. Biophys. Acta 167*, 227.
Engel, P. C., and Dalziel, K. (1969), *Biochem. J. 115*, 621.
Fahien, L. A., and Strmecki, M. (1969), *Arch. Biochem. Biophys. 130*, 456.
Fisher, H. F., Cross, D., and McGregor, L. L. (1962), *Nature (London) 196*, 895.
Fisher, J. R., and Hoagland, V. D. (1968), *Advan. Biol. Med. Phys. 12*, 165.
Frieden, C. (1958), *Biochim. Biophys. Acta 27*, 431.
Frieden, C. (1959a), *J. Biol. Chem. 234*, 809.
Frieden, C. (1959b), *J. Biol. Chem. 234*, 2891.
Frieden, C. (1963a), *Biochem. Biophys. Res. Commun. 10*, 410.
Frieden, C. (1963b), *J. Biol. Chem. 238*, 3286.
Kornberg, A. (1957), *Methods Enzymol. 3*, 878.
Layne, E. (1957), *Methods Enzymol. 3*, 451.
Olson, J. A., and Anfinsen, C. B. (1952), *J. Biol. Chem. 197*, 67.
Olson, J. A., and Anfinsen, C. B. (1953), *J. Biol. Chem. 202*, 841.
Sweeny, J. R., and Fisher, J. R. (1968), *Biochemistry 7*, 561.
Warburg, O., and Christian, W. (1941), *Biochem. Z. 310*, 384.
Wong, J.-T. F., and Hanes, C. S. (1962), *Can. J. Biochem. Physiol. 40*, 763.
Yielding, K. L., and Holt, B. B. (1967), *J. Biol. Chem. 242*, 1079.
Yielding, K. L., and Tomkins, G. M. (1962), *Recent Progr. Horm. Res. 18*, 467.

Tyrosyl and Lysyl Residues Involved in the Reactivity of Catalytic and Regulatory Sites of Crystalline Beef Liver Glutamate Dehydrogenase*

G. di Prisco

ABSTRACT: Beef liver glutamate dehydrogenase has been chemically modified with 1-fluoro-2,4-dinitrobenzene, a reagent of functional groups of proteins. Dinitrophenylation has been shown to cause both inactivation and desensitization of the enzyme to ADP activation and GTP inhibition: these effects could be prevented by the presence of NAD (which protected the active site), ADP, and GTP (each of which had been previously shown to afford selective protection to its specific regulatory site). Reacting glutamate dehydrogenase under these conditions yielded a dinitrophenylated enzyme, which retained essentially the same kinetic behavior as that of native glutamate dehydrogenase. The results of a second dinitrophenylation with [^{14}C]1-fluoro-2,4-dinitrobenzene, performed under conditions of partial protection of the enzyme, in which no more than one site at a time has been exposed to the action of the reagent, have shown that site reactivity is lost concomitantly with dinitrophenylation of nine amino acid residues per site per mole of active oligomer. Following total hydrolysis, electrophoretic and chromatographic identification of the radioactive dinitrophenylated amino acids has indicated lysyl and tyrosyl, in the ratio of approximately two to one, as the only residues whose chemical modification causes loss of activity and/or allosteric response. One can therefore suggest that the reactivity of the active and the two regulatory sites of the active oligomer of beef liver glutamate dehydrogenase is dependent on three separate but identical sets of amino acid residues, each composed of six lysyl and three tyrosyl residues.

In a previous communication (di Prisco, 1967), it was reported that reacting crystalline beef liver glutamate dehydrogenase (L-glutamate–NAD(P) oxidoreductase (deaminating), EC 1.4.1.3) with 1-fluoro-2,4-dinitrobenzene (FDNB)[1] caused a time-dependent loss of catalytic activity and of the propensity for allosteric activation by ADP and inhibition by GTP. The presence of the reaction coenzyme NAD during dinitrophenylation prevented the inactivation, and the presence, in addition, of one of the two allosteric modifiers prevented the loss of its specific allosteric effect. Although previous kinetic studies (Frieden, 1963) had supported the view that both allo-

* From the International Laboratory of Genetics and Biophysics, Naples, Italy. *Received July 27, 1970.* Preliminary accounts of these findings were presented at the 4th Meeting of the Federation of the European Biochemical Societies, Oslo, Norway, 1967; 7th International Congress of Biochemistry, Tokyo, Japan, 1967; and Advanced Study Institute on Pyridine Nucleotide Dependent Dehydrogenases, Konstanz, West Germany, 1969.

[1] Abbreviation used is: FDNB, 1-fluoro-2,4-dinitrobenzene.